PHYSICAL REVIEW VOLUME 106, NUMBER 5 JUNE 1, 1957

Determination of Optical Constants and Carrier Effective Mass of Semiconductors*

W. G. SPITZER† AND H. Y. FAN
Purdue University, Lafayette, Indiana
(Received February 18, 1957)

By using reflectivity and absorption measurements in the region 5 to 35 micron, the effect of free carriers on the optical constants has been determined for n- and p-type germanium, silicon, and indium antimonide, and for n-type indium arsenide. The contribution of the free carriers to the electric susceptibility is obtained from the optical constants. A carrier effective mass, m_s, is defined in terms of the susceptibility, and the significance of m_s is considered for four different types of energy band structure. The experimental values of m_s are compared with those calculated by using data from other experiments. Good agreement was found for n- and p-type silicon, n-type germanium, and p-type indium antimonide. In p-type germanium, the susceptibility due to transitions between the overlapping bands in the valence band was taken into account. However, the resulting m_s, for a sample of $\sim 10^{19}$ cm^{-3} impurity concentration, is larger by a factor of 1.8 than that calculated by using cyclotron resonance data. In n-type indium antimonide m_s increases with carrier concentration. If one assumes m_s to be energy-dependent, the shape of the conduction band calculated is consistent with previously reported measurements of the shift of the intrinsic absorption edge with electron concentrations. In the case of n-type indium arsenide, m_s differs from the effective mass reported from thermoelectric measurements but gives good agreement with the values determined from the shift of the intrinsic absorption edge for an impure specimen.

I. INTRODUCTION

THE reflectivity of semiconductors is usually constant over a large spectral region on the long-wavelength side of the intrinsic absorption edge. The value of the reflectivity is close to that which is predicted by the refractive index of the bulk material. However, measurements on semiconductor samples of large carrier concentrations showed variations of reflectivity at long wavelengths.[1] The effect has been interpreted as due to the contributions of free carriers to the electrical susceptibility and conductivity,[2] and is to be distinguished from the residual ray reflectivity bands seen recently in many III-V intermetallic semiconductors.[3]

Both optical constants, the refractive index and the extinction coefficient, can be determined if reflectivity and transmission measurements are made on the same material. From the optical constants obtained for samples of different carrier concentrations, the conductivity and the electrical susceptibility of free carriers can be evaluated. The susceptibility is appreciable where the reflectivity shows variations. If the radiation frequency is large compared to the collision frequency, $1/\tau$, of the carriers, the susceptibility should be independent of τ and depends solely on the structure of the energy band, aside from the carrier concentration. An effective mass can be defined in terms of the susceptibility, which characterizes the energy band. The measurements can be made with ease, and the interpretation is straight forward and does not involve uncertain assumptions. A number of semiconductors have been investigated this way, including n- and p-type materials of germanium, silicon, and indium antimonide as well as n-type arsenide. The results will be reported and compared with data which are available for the semiconductors from other experiments. For indium arsenide, the shift of the intrinsic absorption edge with carrier concentration has also been measured. Such data, which are compared with the results of optical constants measurements, have not been reported previously.

II. THEORY

(A) Susceptibility, Conductivity, and Effective Mass of Free Carriers

If the applied electric field varies with time according to

$$\mathcal{E}_x = \mathcal{E}_0 e^{i\omega t},$$

then it can be shown that the solution of the Boltzmann equation for the current density in the x direction may be written[4]

$$j_x = -\frac{2}{(2\pi)^3}\frac{e^2}{\hbar}\left[\mathcal{E}_x \int \frac{\tau v_x}{1+(\omega\tau)^2}\frac{\partial f_0}{\partial k_x}d\Omega_k - \frac{\partial \mathcal{E}_x}{\partial t}\int \frac{\tau^2 v_x}{1+(\omega\tau)^2}\frac{\partial f_0}{\partial k_x}d\Omega_k\right],$$

where $2/(2\pi)^3$ is the density of states in wave number vector, $\mathbf{k}$, space, τ is the carrier relaxation time, f_0 is

---

* This work was supported by an Office of Naval Research contract.

† Based in part on a Ph.D. thesis submitted to Purdue University.

[1] K. Lark-Horovitz and K. W. Meissner, Phys. Rev. 76, 1530 (1949).

[2] H. Y. Fan and M. Becker, "The Infrared Optical Properties of Silicon and Germanium," *Symposium Volume of the Reading Conference* (Butterworth Publishing Company, London, 1951).

[3] W. Spitzer and H. Y. Fan, Phys. Rev. 99, 1893 (1955); also Picus, Burstein, and Hennis, Bull. Am. Phys. Soc. Ser. II, 2, 66 (1951).

[4] H. Y. Fan, *Solid State Physics*, edited by F. Seitz and D. Turnbull (Academic Press, Inc., New York, 1955), Vol. 1, p. 352, Eq. (19.3).

the occupation probability, $d\Omega_k = dk_x dk_y dk_z$ is the volume element in wave number vector space, and v_x is the electron velocity in the direction x. We shall consider crystals of cubic symmetry. Writing

$$j_x = \sigma \mathcal{E}_x + \chi_c \partial \mathcal{E}_x / \partial t,$$

the conductivity, σ, and the electric susceptibility, χ_c, given by

$$\sigma = -\frac{e^2}{\hbar} \int \frac{\tau v_x}{1+(\omega\tau)^2} \frac{\partial f_0}{\partial k_x} \frac{2}{(2\pi)^3} d\Omega_k, \tag{1}$$

and

$$\chi_c = \frac{e^2}{\hbar} \int \frac{\tau^2 v_x}{1+(\omega\tau)^2} \frac{\partial f_0}{\partial k_x} \frac{2}{(2\pi)^3} d\Omega_k \tag{2}$$

should be independent of the direction, x, of the electric field. For the cases of interest, $(\omega\tau)^2 \gg 1$, giving

$$\chi_c = \frac{e^2}{\hbar\omega^2} \int v_x \frac{\partial f_0}{\partial k_x} \frac{2}{(2\pi)^3} d\Omega_k, \tag{3}$$

which is independent of τ. Integrating by parts, the integral in (3) becomes

$$-\int \frac{\partial v_x}{\partial k_x} f_0 d\Omega_k + \int [v_x f_0]_{k_x=-\infty}^{k_x=+\infty} dk_y dk_z.$$

The second term is zero. Using $v_x = (1/\hbar)\partial E/\partial k_x$, where E is the energy of the carrier, we have

$$\chi_c = \frac{e^2}{\omega^2\hbar^2} \int \frac{\partial^2 E}{\partial k_x^2} \frac{2}{(2\pi)^3} f_0 d\Omega_k, \tag{4}$$

where x is an arbitrary direction in the crystal. We note that the same result can be deduced from the quantum-mechanical treatment.[5]

While the conductivity depends essentially on τ, the susceptibility in the range of $(\omega\tau)^2 \gg 1$ does not involve τ and depends only on the structure of the energy band.

We shall define an effective mass in terms of χ_c,

$$\chi_c = -Ne^2/\omega^2 m_s, \tag{5}$$

where N is the carrier concentration, and consider the significance of m_s for four different types of band structure.

(a) The surfaces of constant energy are spherical;

$$E = \hbar^2 k^2 / 2m^*.$$

It follows from (4) and (5) that

$$m_s = m^*. \tag{6}$$

(b) Each surface of constant energy consists of several ellipsoids, as in the conduction bands of germanium and silicon. Near any one of the minima in the band, the energy can be expressed by

$$E = \frac{\hbar^2}{2}\left(\frac{k_1^2}{m_1} + \frac{k_2^2}{m_2} + \frac{k_3^2}{m_3}\right),$$

where $\mathbf{k}_1$, $\mathbf{k}_2$, and $\mathbf{k}_3$ are along the principal axes of the ellipsoid. In this case $\partial^2 E/\partial k_x^2$ is independent of $|\mathbf{k}_1|$, $|\mathbf{k}_2|$, and $|\mathbf{k}_3|$, and the susceptibility of carriers in the one valley is, according to (4),

$$\frac{e^2}{\omega^2} \frac{n}{\hbar^2} \frac{\partial^2 E}{\partial k_x^2} = -\frac{e^2}{\omega^2} n \left[\frac{\cos^2(\mathbf{k}_x,\mathbf{k}_1)}{m_1} + \frac{\cos^2(\mathbf{k}_x,\mathbf{k}_2)}{m_2} + \frac{\cos^2(\mathbf{k}_x,\mathbf{k}_3)}{m_3}\right], \tag{7}$$

where n is the concentration of carriers in the valley. χ_c for the crystal is obtained by summing the contributions from all the valleys in the energy band. Because of the cubic symmetry, χ_c is independent of the orientation of the crystal with respect to $\mathbf{k}_x$, and is identical to the value averaged over all possible directions of $\mathbf{k}_x$. We can also take the average of (7) over the directions of $\mathbf{k}_x$ and multiply the result by the number of valleys. The result is

$$\chi_c = \frac{-e^2 N}{\omega^2} \frac{1}{3}\left(\frac{1}{m_1} + \frac{1}{m_2} + \frac{1}{m_3}\right). \tag{8}$$

Comparing with (5), we get

$$\frac{1}{m_s} = \frac{1}{3}\left(\frac{1}{m_1} + \frac{1}{m_2} + \frac{1}{m_3}\right). \tag{9}$$

As is seen, f_0 enters only into the determination of N and the result (9) does not depend upon the distribution function.

(c) In germanium and silicon the valence band is composed of 3 overlapping bands. The maxima of two bands meet at $\mathbf{k}=0$ and the maximum of the third band is also at $\mathbf{k}=0$ but lies at a lower energy. Under normal conditions the carriers are concentrated in the two higher bands, and the susceptibility will be taken as the sum of that of carriers in each band. Approximating the surfaces of constant energy by spheres, we have

$$\chi_c = \frac{-N_1 e^2}{\omega^2 m_1} + \frac{-N_2 e^2}{\omega^2 m_2},$$

where N_1, N_2, m_1, and m_2 are the carrier concentrations and effective masses in the two bands, respectively. Using the additional relations,

$$N_1/N_2 = \left(\frac{m_1}{m_2}\right)^{\frac{3}{2}} \quad \text{and} \quad N_1 + N_2 = N,$$

[5] H. Wilson, *Theory of Metals* (Cambridge University Press, Cambridge, 1936), p. 131.

we obtain by comparison to (5)

$$\frac{1}{m_s}=\frac{m_1^{\frac{1}{2}}+m_2^{\frac{1}{2}}}{m_1^{\frac{3}{2}}+m_2^{\frac{3}{2}}}. \tag{10}$$

(d) It has been assumed in the above cases that the mass parameters in the $(E,\mathbf{k})$ relationship are constant, independent of energy. Because of some experimental results to be pointed out, it is of interest to consider the case of spherical constant-energy surfaces,

$$E=\hbar^2k^2/2m^*(k),$$

where $m^*(k)$ is a function of the magnitude of $\mathbf{k}$. Using Eq. (3) with $v_x=(1/\hbar)(\partial E/\partial k_x)$ and replacing v_x^2 by $\frac{1}{3}v^2$, we have

$$\chi_c=\frac{2}{(2\pi)^3}\frac{e^2}{3\omega^2}\int v^2\frac{\partial f_0}{\partial E}d\Omega_k.$$

The quantity $d\Omega_k$ can be written as

$$[dS_{\mathbf{k}}(E)/\mathrm{grad}_{\mathbf{k}}E]dE,$$

where $S_{\mathbf{k}}(E)$ is the surface in $\mathbf{k}$ space corresponding to the energy E. Integrating first over $S_{\mathbf{k}}(E)$, then over E, we obtain

$$\chi_c=-\frac{e^2}{\omega^2}\frac{2}{(2\pi)^3}\frac{1}{3\hbar}\bar{v}^{\zeta}S_{\mathbf{k}}(\zeta),$$

where ζ is the Fermi energy and $\bar{v}^{\zeta}$ is the velocity averaged over the Fermi surface. For spherical constant-energy-surfaces:

$$S_{\mathbf{k}}(\zeta)=4\pi k^{\zeta 2},\quad N=\frac{2}{(2\pi)^3}\frac{4\pi k_\zeta^3}{3},\quad\text{and}\quad \bar{v}^{\zeta}=\frac{1}{\hbar}\left|\frac{\partial E}{\partial k}\right|_\zeta.$$

Comparing the expressing of χ_c with (5), we see that

$$\frac{1}{m_s}=\frac{1}{\hbar^2k_\zeta}\left|\frac{\partial E}{\partial k}\right|_\zeta. \tag{11}$$

It should be noted that this value is not the same as

$$m^*(k_\zeta)=\hbar^2k_\zeta^2/\zeta.$$

(B) Electric Susceptibility Due to Interband Transitions

Thus far our attention has been restricted to what might be called the conductive effect of carriers. When an energy band is composed of overlapping bands, carrier transitions between the bands may contribute to the susceptibility as well as the absorption of radiation. Such absorption has been observed in p-type germanium.[6] The susceptibility associated with electron transitions from a band v to a band j is given by[7]

$$\chi_v=\frac{e^2}{4\pi^2m}\sum_{\mathbf{k}}\frac{f_{jv\mathbf{k}}}{\nu_{jv\mathbf{k}}^2-\nu^2}, \tag{12}$$

where $\mathbf{k}$ is the wave number vector, $h\nu_{jv\mathbf{k}}$ is the energy difference between the state at $\mathbf{k}$ in the band v and the state in the band j at the same $\mathbf{k}$, and $f_{jv\mathbf{k}}$ is the oscillator strength for the transition. Expression (12) may be written as

$$\chi_v=\frac{1}{\pi^2}\int\frac{\sigma_v(\nu_{jv\mathbf{k}})}{\nu_{jv\mathbf{k}}^2-\nu^2}d\nu_{jv\mathbf{k}}, \tag{13}$$

where

$$\sigma_v(\nu)=(e^2/4m)f_{jv}(\nu)\eta_v(\nu) \tag{14}$$

is the conductivity which characterizes the absorption associated with the transitions. $\eta_v(\nu_{jv\mathbf{k}})d\nu_{jv\mathbf{k}}$ gives the number of states of the band v per unit volume, for which the transition frequency lies in the range between $\nu_{jv\mathbf{k}}$ and $\nu_{jv\mathbf{k}}+d\nu_{jv\mathbf{k}}$. If the absorption coefficient, α_v, associated with such transitions and refractive index, n, of the crystal are known, then σ_v can be obtained, according to

$$\sigma_v=(cn/4\pi)\alpha_v \tag{15}$$

and the susceptibility χ_v can be calculated by using (13).

III. EXPERIMENTAL METHOD

All optical measurements were made at room temperature (297°K) and the specimens used were all single crystals with the exception of the indium arsenide. The reflectivity of the material of refractive index n and extinction coefficient κ is given by

$$R=\frac{(n-1)^2+\kappa^2}{(n+1)^2+\kappa^2}. \tag{16}$$

The transmission, in the absence of interference fringes, is given by[2]

$$T=\frac{(1-R)^2e^{-\alpha x}}{1-R^2e^{-2\alpha x}}, \tag{17}$$

where α is the linear absorption coefficient and x is the sample thickness. α is related to κ by

$$\alpha=4\pi\kappa/\lambda. \tag{18}$$

By using these relations, n and κ can be determined from measurements of R and T. The susceptibility can be calculated according to

$$\epsilon=\epsilon_0+4\pi\chi_c=n^2-\kappa^2, \tag{19}$$

where ϵ_0 is the dielectric constant in the absence of any contribution from free carriers. ϵ_0 may be obtained from a measurement of R on a pure sample.

The reflectivity is measured using specimens with polished surfaces and a thickness such that $\alpha x\gg 1$. The sample is then reduced in thickness until it is convenient for transmission measurements. In most cases this thickness is of the order of 10 microns. The thickness is measured using transmission interference fringes at wavelengths slightly longer than the intrinsic absorption edge. Since in almost all of the materials the carrier

[6] Kaiser, Collins, and Fan, Phys. Rev. **91**, 1380 (1953).
[7] See H. Y. Fan, Repts. Progr. in Physics **XIX**, 107 (1956).

absorption increases with increasing wavelength, the fringes are measured in a region with relatively high transmission.

The first experimental test of the validity of (3) is made by checking the proportionality between χ_c and λ^2. The condition, $\omega^2\tau^2 \gg 1$, should be satisfied if this relationship is observed. From (5) and the experimental values of χ_c the quantity N/m_s is obtained. The determination of the carrier concentration is made from Hall measurements on the same specimens which are used for the optical measurements. In all cases except silicon, the Hall coefficient was the same at 297°K and 77°K. If the expression

$$R_H = \pm 1/Ne \tag{20}$$

is used where R_H is the value measured at 77°K, then the Fermi energy may be calculated using

$$N = \frac{4\pi(2m_d kT)^{\frac{3}{2}}}{h^3} \int_0^\infty \frac{x^{\frac{1}{2}}dx}{1+e^{x-\zeta^*}}, \tag{21}$$

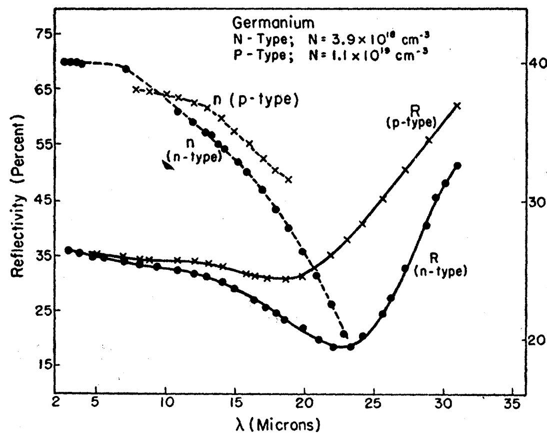

FIG. 1. Reflectivity and refractive index as functions of wavelength for n-type germanium and p-type germanium samples, where N is the majority carrier concentration.

where m_d is the density-of-states mass, k is the Boltzmann constant, and ζ^* is the Fermi level divided by kT. In all cases ζ is found to be at least $7kT$ inside the conduction or valence band. Therefore, (20) should yield a good estimate of N at 77°K. For all samples, except those of silicon, the carrier concentration at 297°K is taken to be the same as the value found for 77°K. In the case of silicon the Hall coefficient measured at 297°K has to be used. The expression (20) is used to calculate N. It will be shown that this value of N leads to a value of m_s which is in excellent agreement with the data of cyclotron resonance experiments, according to (9) or (10).

The Hall coefficient and the resistivity may be combined to give an estimate of a relaxation time τ_H;

$$R_H/\rho = (e/m_s)\tau_H. \tag{22}$$

This value, τ_H, should indicate the order of magnitude

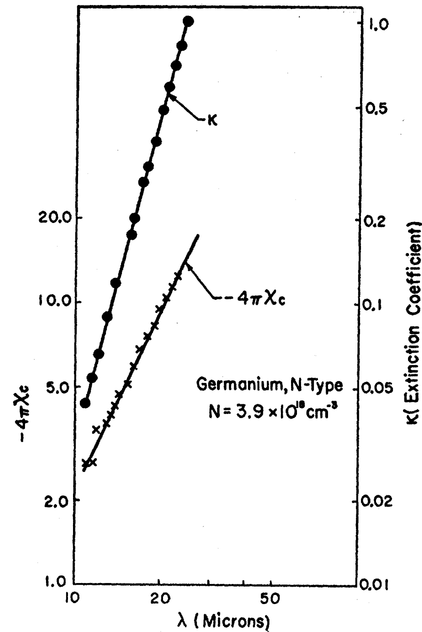

FIG. 2. Extinction coefficient and free carrier susceptibility as a function of wavelength for the n-type germanium sample of Fig. 1. The straight line through the $-4\pi\chi_c$ points is drawn with a slope of 2.

of the collision time of carriers. One may check the condition $\omega^2\tau_H^2 \gg 1$ using the frequencies for which χ_c is determined.

IV. RESULTS AND DISCUSSION

n-Type Germanium

The spectral curve for the room temperature reflectivity of an arsenic-doped germanium sample is shown in Fig. 1. The absorption coefficient, α, and extinction coefficient, κ, have been determined from transmission measurements and κ is shown in Fig. 2. The refractive

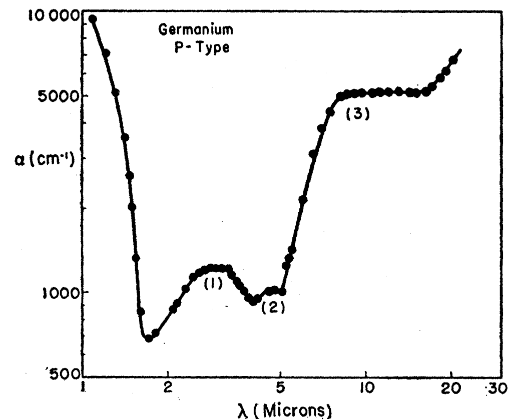

FIG. 3. Absorption coefficient, α, vs wavelength for the p-type germanium sample of Fig. 1. The numbers (1), (2), and (3) indicate the absorption bands attributed to interband transitions within the valence band.

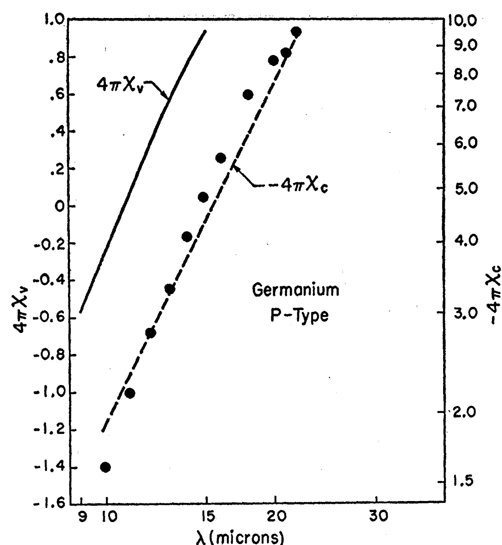

FIG. 4. The susceptibility for interband transitions, χ_v, as a function of wavelength for the p-type germanium sample of Fig. 1 is given by the solid curve. The susceptibility, χ_c, is given by the points.

index, n, determined as described previously is also given in Fig. 1. The refractive index as a function of wavelength was also determined for this sample using transmission interference fringes measured to 15 microns. The results agree within 5% with those obtained from transmission and reflectivity data.

Several of the characteristics of the reflectivity curve become clear. The large decrease in the reflectivity beyond about 10 microns is due to a decreasing refractive index; the κ^2 term in (16) is negligible until approximately 18 microns. In this spectral region (17) and (19) become

$$R=(n-1)^2/(n+1)^2 \quad \text{and} \quad \epsilon=n^2.$$

Beyond 18 microns, the rapidly increasing κ is no longer negligible in the reflectivity expression (16). The effect of κ is to increase the reflectivity. Because of the increasing absorption, it was not possible to measure the transmission at wavelengths over 24 microns, therefore,

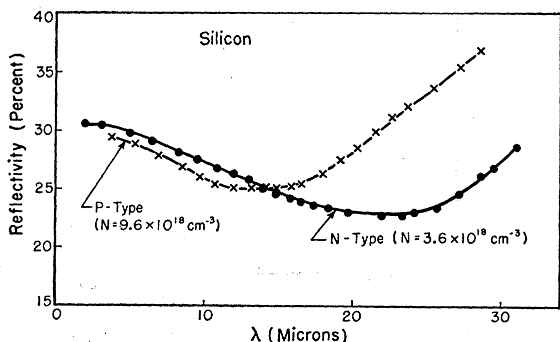

FIG. 5. Reflectivity *vs* wavelength for n-type and p-type silicon samples, where N is the majority carrier concentration.

the values of n and κ could be determined reliably only for $\lambda<24$ microns.

A plot of $\ln(-4\pi\chi_c)$ *vs* $\ln\lambda$ is given in Fig. 2. As is seen, the wavelength squared dependence of χ_c is quite well satisfied for the sample. The value of m_s obtained from the susceptibility measurements is $0.15m$, where m is the free electron mass. This result is in reasonably good agreement with the value of $m_s=0.12m$ obtained from (9) by using cyclotron resonance data.[8]

It is also of interest to note that the slope of the absorption curve is approximately 2.9, which is considerably larger than the 2.0 predicted by Drude theory. This effect has been reported previously.[9]

(B) p-Type Germanium

The interpretation of the measurements for p-type germanium is complicated by the presence of interband transitions of the type considered in Sec. (IIB). The reflectivity and absorption coefficient curves for a gallium-doped germanium sample are shown in Figs. 1 and 3. The 3 bands seen in the absorption coefficient

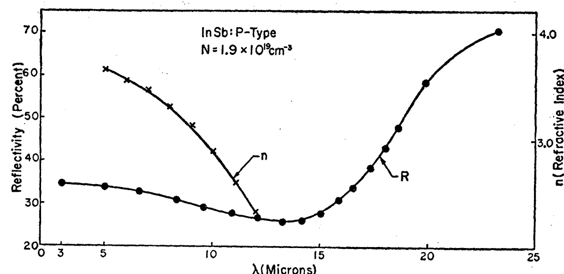

FIG. 6. Reflectivity and refractive index *vs* wavelength for a p-type indium antimonide sample.

curve has been attributed to the interband transitions.[10] The rise at the long-wavelength end of the curve[11] is due to the ordinary conduction effect of the free carriers.

When one uses the values of n deduced from the reflection and transmission measurements, the conductivity $\sigma_v(\nu)$ associated with the interband transitions can be calculated from the absorption coefficient. The susceptibility χ_v can be then calculated using (13). The results are given in Fig. 4. The measured values of n and κ determine the total susceptibility of free carriers. Subtracting from it χ_v, we obtain χ_c which is also given in Fig. 4 for various wavelengths. The dashed curve is drawn proportional to λ^2 and so as to give the best fit. The curve gives $m_s=0.50m$. On the other hand, Eq. (10) gives $m_s=0.27m$ using the cyclotron resonance values of m_1 and m_2.[8] The discrepancy seems to indicate that a high impurity concentration, 1.1×10^{19} cm^{-3} in the sample used, changes the values of m_s.

[8] Dexter, Zeiger, and Lax, Phys. Rev. **104**, 637 (1956).
[9] Fan, Spitzer, and Collins, Phys. Rev. **101**, 566 (1954).
[10] A. H. Kahn, Phys. Rev. **97**, 1647 (1955).
[11] E. Johnson and W. Spitzer, Phys. Rev. **94**, 1415 (1954).

(C) n-Type and p-Type Silicon

Both the n-type and p-type silicon measurements are treated in the same manner as the n-type germanium. Although silicon has a valence band structure similar to that of germanium, the p-type silicon carrier absorption spectrum does not show any band structure up to 40 microns. Figure 5 shows the reflectivity curves for the silicon samples. The values of m_s are $0.27m$ for the n-type silicon and $0.37m$ for the p type as determined from (5). These values are to be compared to the corresponding values of $0.26m$ and $0.39m$.[8] The agreement in both cases is quite good.

(D) p-Type Indium Antimonide

The reflectivity, refractive index, absorption, and susceptibility curves for a zinc-doped indium antimonide sample are shown in Figs. 6 and 7. It is usually found in semiconductors that the free-carrier absorption increases with increasing wavelength. Although the absorption in p-type indium antimonide shows little wavelength dependence, it is assumed that the absorption is due to the conduction effect of free carriers. The susceptibility χ_c obtained on this assumption does show the λ^2 dependence. The value $m_s=0.20m$ is obtained which is in good agreement with the cyclotron resonance value of $0.18m$.[12]

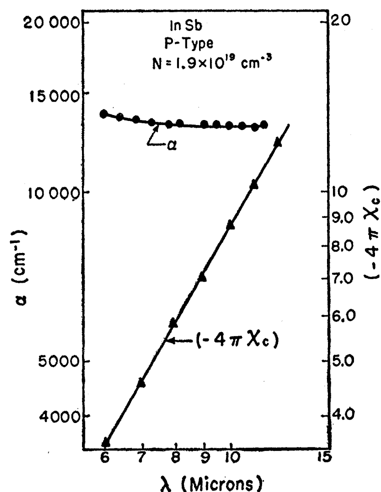

FIG. 7. Absorption coefficient, α, and susceptibility, χ_c, *vs* wavelength for the p-type indium antimonide sample of Fig. 6.

(E) n-Type Indium Antimonide

The measurements on n-type indium antimonide yield several interesting results. Figure 8 shows the spectral dependence of the reflectivity for five tellurium-doped samples of different carrier concentrations. The striking difference between these reflectivity curves and those previously shown are the extremely deep minima in the curves of Fig. 8. The depth of the minimum is controlled by the extinction coefficient κ. It is clear from (16) that as long as κ^2 is small, the reflectivity will reach a low value at a wavelength corresponding to $n\simeq 1$. Whether or not κ^2 will be small near this wavelength depends on the value of τ. Whereas σ is determined by τ, χ_c is independent of it. Both σ and χ_c increase in magnitude with the wavelength. With a large value of τ, σ may be low enough to give small values of κ, while $-4\pi\chi_c$ becomes sufficiently large

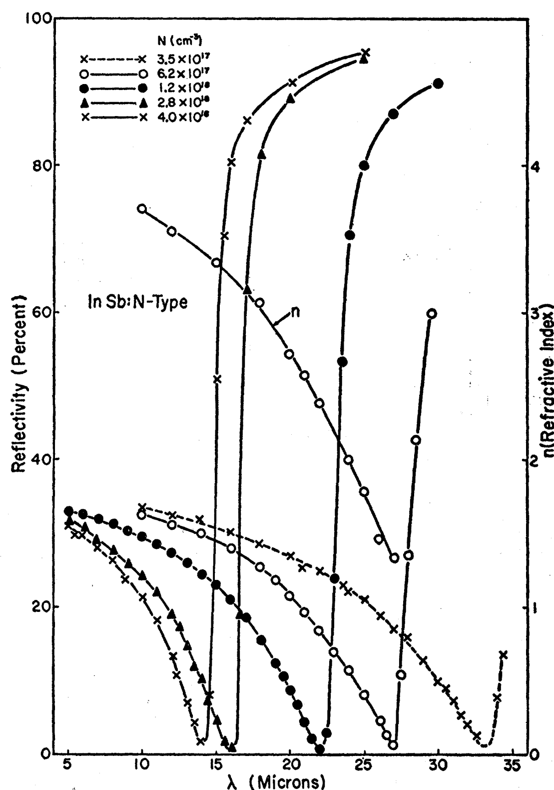

FIG. 8. Reflectivity *vs* wavelength for five n-type indium antimonide samples. The refractive index curve labeled n is for the sample with $N=6.2\times10^{17}$ cm^{-3}.

TABLE I. A summary of the experimental data from the present measurements. The last column contains the values for effective mass of free carriers obtained from other measurements.

Material	Type	Present measurements N	τ_H	m_s/m	Effective mass from other measurements m_s/m
Germanium	n	3.9×10^{18}	4.4×10^{-14}	0.15	0.12[a]
	p	1.1×10^{19}	6.2×10^{-14}	0.50	0.27[a]
Silicon	n	3.6×10^{18}	2.7×10^{-14}	0.27	0.26[a]
	p	9.6×10^{18}	1.0×10^{-14}	0.37	0.39[a]
InSb	p	1.9×10^{19}	3.0×10^{-14}	0.20	0.18[b]
	n	3.5×10^{17}	4.7×10^{-13}	0.023	0.015[c] and
	n	$6.2\ (5)\times10^{17}$	4.0×10^{-13}	0.029	0.03[d]
	n	1.2×10^{18}	4.0×10^{-13}	0.032	
	n	2.8×10^{18}	3.2×10^{-13}	0.040	
	n	4.0×10^{18}	2.6×10^{-13}	0.041	
InAs	n	2.4×10^{17}	2.7×10^{-13}	0.030	0.064[e]
	n	1.4×10^{18}	3.8×10^{-13}	0.033	

[a] See reference 8.
[b] See reference 12.
[c] See reference 13.
[d] See reference 14.
[e] See reference 16.

[12] Dresselhaus, Kip, Kittel, and Wagoner, Phys. Rev. 98, 556 (1955).

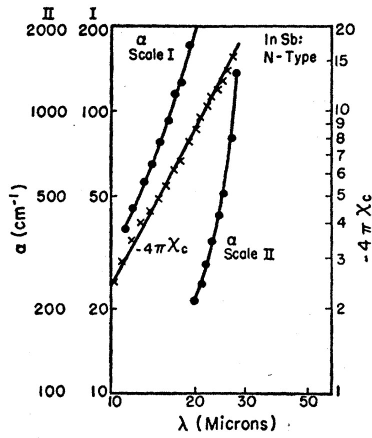

FIG. 9. Absorption coefficient, α, and susceptibility, χ_c, *vs* wavelength for the n-type indium antimonide sample of Fig. 9, where $N=6.2\times10^{17}$ cm^{-3}.

to reduce the dielectric constant and the refractive index. The minimum value of reflectivity will, therefore, be low. This point is illustrated in Table I where it is seen that the values of τ_H determined from (22), are an order of magnitude larger for n-type indium antimonide than for any of the other materials discussed thus far. The spectral curves for the refractive index, absorption coefficient, and susceptibility for one of the samples are seen in Figs. 8 and 9. It is indeed seen that κ^2 is negligible in (17) until the minimum reflectivity is reached.

The very low value of the minimum in the reflectivity curve also makes it unnecessary to make the transmission measurements to determine χ_c. When the value of R is small at the minimum, then $\kappa^2 \ll 1$ according to (16). Since κ decreases with decreasing wavelength, it can be neglected on the short wavelength side of the minimum reflectivity.

The value of m_s has been determined for each of the samples in Fig. 8. It is not a constant but varies from $m_s=0.023m$ for the sample of smallest carrier concentration to $m_s=0.041m$ for the largest concentration. Figure 10 shows a plot of m_s/m as a function of carrier concentration. While it may be expected that the introduction of impurities could alter the shape of the conduction band, the observed variation of m_s is considerably larger than we would expect. It is believed that the conduction band in indium antimonide has spherically

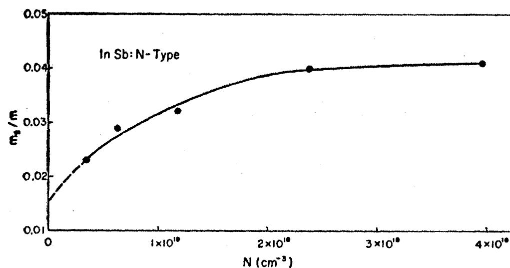

FIG. 10. The dots represent the measured values of m_s/m as a function of electron carrier concentration in n-type indium antimonide.

constant energy surfaces. If one takes m_s as a function of energy, Eq. (11) must be used for its interpretation, all samples being degenerate. By using the relation

$$N=\frac{2}{(2\pi)^3}\frac{4\pi k_\zeta^3}{3},$$

Eq. (11) may be written as

$$\left|\frac{\partial E}{\partial k}\right|_\zeta=\frac{\hbar^2(3\pi^2N)^{\frac{1}{3}}}{m_s}. \tag{23}$$

Cyclotron resonance measurements made at room temperature give an effective cyclotron mass of $0.15m$.[13] The sample used should be intrinsic at room temperature with an electron concentration of the order of 10^{16} cm^{-3}. The electrons are not degenerate and the effective cyclotron mass is not given by (11). However,

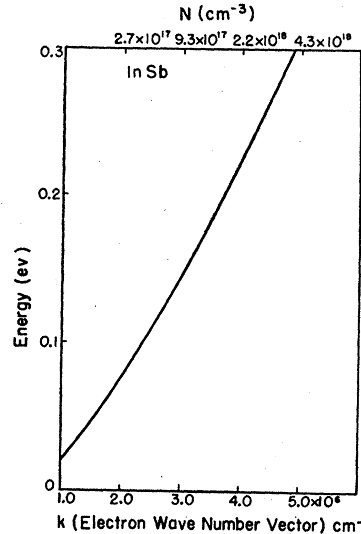

FIG. 11. Conduction band energy of n-type indium antimonide *vs* magnitude of wave number vector, $\mathbf{k}$, and carrier concentration, N.

we note that the value falls not far from the extrapolation of the curve of m_s in Fig. 10. Using Fig. 10, Eq. (23) may be integrated. A plot of E *vs* k for the conduction band obtained in this way is shown in Fig. 11. The values of E at small N, in Fig. 11, are affected to some extent by the extrapolation of the curve in Fig. 10 and are therefore not too reliable.

It is well known that the intrinsic absorption edge of indium antimonide shifts to shorter wavelengths as the electron carrier concentration increases to larger values. These results have been previously analyzed[14] on the basis of an effective mass of $0.03m$ independent of energy. It is of interest whether the energy dependent effective mass determined from the susceptibility is in contradiction with the experimental edge measurements. The dots in Fig. 12 give $h\nu$ *vs* $\mathbf{k}$ for a number of samples, where $h\nu$ is the experimental value

[13] Burstein, Picus, and Gebbie, Phys. Rev. **103**, 825 (1956).
[14] W. Kaiser and H. Y. Fan, Phys. Rev. **98**, 966 (1955).

of the photon energy for an absorption coefficient of 300 cm^{-1} and k is the electron wave number determined from N. The expression for the energy,[14] $h\nu$, corresponding to an absorption coefficient, α, is

$$h\nu(\alpha)=E_g+\left(1+\frac{m_e^*}{m_h^*}\right)\left[\zeta-kT\ln\left(\frac{\alpha_0-\alpha}{\alpha}\right)\right], \quad (24)$$

where E_g is the energy gap, k is the Boltzmann constant, and α_0 is the absorption coefficient in a pure sample at the same $h\nu$. The derivation of this expression assumes direct transitions across the forbidden energy gap. The Fermi energy, ζ, may be taken from Fig. 11. Using α_0 and α from room temperature absorption graphs, $(h\nu-E_g)$ may be calculated. The crosses on Fig. 12 are the calculated values of $(h\nu-E_g)$ taking E_g to be 0.18 ev. The theoretical points are in reasonable

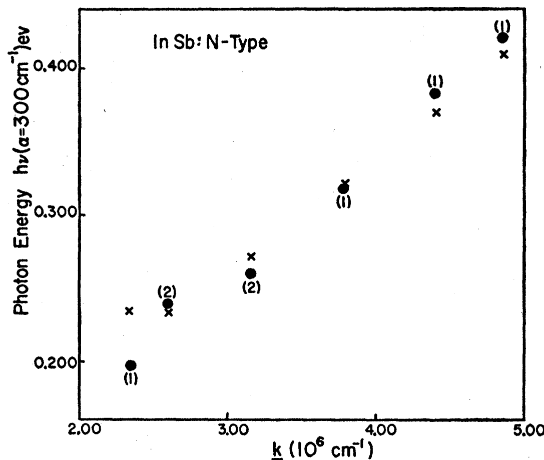

FIG. 12. Photon energy, $h\nu$, for an absorption coefficient $\alpha=300$ cm^{-1} of the n-type indium antimonide intrinsic absorption edge as a function of the magnitude of the electron wave-number vector, $\mathbf{k}$, at the Fermi energy. The dots are experimental values taken from the data of (1) Kaiser and Fan[14] and (2) G. Gobeli, Purdue University (unpublished). The crosses are the calculated values.

agreement with the experimental data given by the dots. The value $E_g=0.18$ ev, chosen for best fit, is in good agreement with previous estimates of E_g at room temperature.[15]

(F) n-Type Indium Arsenide

Reflectivity curves for two polycrystalline n-type indium arsenide samples as well as one p-type sample are shown in Fig. 13. The n-type curves are quite similar to those for n-type indium antimonide. However, although the carrier concentrations of the two samples differ by a factor of ~ 6, the m_s is substantially the same for both samples. The values obtained are $m_s=0.030m$ for the sample of lower carrier concentration and $m_s=0.033m$ for the second sample. We shall assume therefore that $m_s=m^*$ is energy independent. Recent thermoelectric measurements of indium arsenide yield an electron effective mass of[16] $0.064m$ between 500 and 800°K which is considerably higher than our value. Although our samples have much higher impurity concentrations, the insensitiveness of m^* to the impurity concentration seems to rule out this difference as the

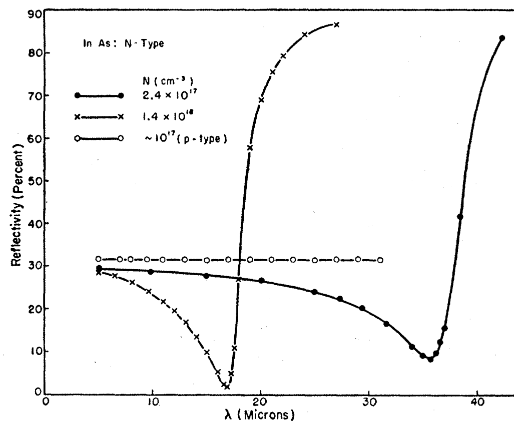

FIG. 13. Reflectivity vs wavelength for two n-type indium arsenide samples as well as a p-type sample of a sufficiently small hole concentration such that $\chi_c \sim 0$ for the wavelengths used.

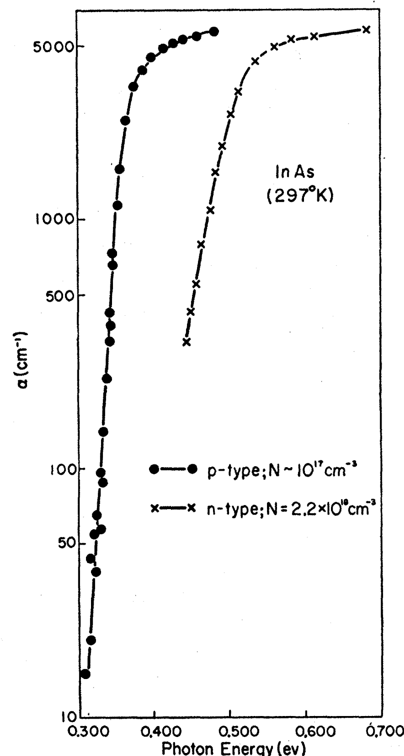

FIG. 14. The room temperature intrinsic absorption edge as a function of photon energy for two indium arsenide samples.

[15] M. Tannenbaum and H. B. Briggs, Phys. Rev. **91**, 1561 (1953); also reference 14.

[16] H. Weiss, Z. Naturforsch. **11a**, 131 (1956).

cause of discrepancy. Moreover, the Fermi energies of the samples used here correspond to temperatures greater than 500°K.

Also, similar to the case of n-type antimonide, the intrinsic edge for impure n-type indium arsenide samples is shifted to higher energy. Figure 14 shows the room temperature intrinsic edge as a function of photon energy for a p-type sample of low carrier concentration and an n-type sample with a carrier concentration of 2.20×10^{18} cm^{-3}. By using (24) with $E_g=0.33$ ev[17] $h\nu(\alpha)=0.470$ ev, and $m_e^*/m_h^*\sim0.1$, ζ may be determined for the impure sample. From ζ and N, m^* is calculated to be $0.035m$. The value of $E_g=0.33$ ev obtained from either photovoltaic effect or optical absorption is subject to uncertainty, depending on what level of the effect is taken to be the threshold. As can be seen in Fig. 14, the value of E_g can be taken to be 0.31 ev, in which case we would obtain $m^*=0.031m$ in substantial agreement with the values given by the susceptibility.

Table I summarizes the results obtained for the various semiconductors investigated. Available data on effective mass given by other experiments are given for comparison. The relaxation times, τ_H, are determined from the room temperature electrical measurements and Eq. (22).

Measurements of the optical constants provides a simple method of determining the effective mass of carriers. However, in cases where there is more than one band of spherical constant energy surfaces or a band in which the constant energy surfaces are not spherical, the value m_s obtained is an average and the individual mass parameters cannot be determined. Another limitation is the necessity of using rather large carrier concentrations and, therefore, large impurity concentrations, which may affect the effective mass to some extent. For samples of smaller carrier concentrations, measurements have to be made at longer wavelengths.

[17] R. M. Talley and D. P. Enright, Phys. Rev. **95**, 1092 (1954); also F. Oswald, Z. Naturforsch. **10**, 927 (1955).

PHYSICAL REVIEW VOLUME 106, NUMBER 5 JUNE 1, 1957

Stress in Evaporated Ferromagnetic Films

J. ROSS MACDONALD
Texas Instruments Incorporated, Dallas, Texas
(Received February 8, 1957)

Ferromagnetic resonance and oscillation magnetometer measurements on a thin evaporated nickel film annealed in a magnetic field are described. Observations of the dependence of the resonant field magnitude on the angle in the plane of the film between the direction of the magnetic field during annealing and the static resonance field direction show that magnetic annealing produced a preferred magnetic axis in the plane of the film. The good agreement between theory and experiment allows one to establish that the film had bulk-nickel g and saturation magnetization values, a large isotropic tension in the plane, and a lesser uniaxial compression in the plane in the direction of the preferred magnetic axis. In the light of these results, it is suggested that part of the discrepancy between theory and ferromagnetic resonance experiments found recently by Conger and Essig for the dependence of saturation magnetization on evaporated film thickness may have arisen from their omission of stress corrections to the resonance condition. Further, part of the difference between film switching times derived from resonance line widths and those directly measured on the same films by these authors may have been caused by the narrowing of ferromagnetic line widths for thin films, as compared with bulk material, produced by the strong dependence on resonant absorption of power transmission entirely through sufficiently thin films.

FERROMAGNETIC resonance and oscillation magnetometer[1–3] measurements on films or disks afford a powerful means of determining accurate g values[1,3,4] and of investigating the dependence of saturation magnetization,[1,3] magnetocrystalline anisotropy,[5,6] and stress[1,3,4,6] on film parameters.

It has recently been shown that thin alloy films evaporated and annealed in a magnetic field lying in the plane of the film show rectangular hysteresis loops[7] and are useful for very fast switching and storage applications.[7–9] The magnetic field causes the films to develop a preferred magnetic axis or uniaxial anisotropy in the film plane. An applied magnetic field can then switch the film magnetization from a parallel to antiparallel orientation along the magnetic axis and vice versa.

This current interest in evaporated films has suggested that the use of the above measuring techniques be illustrated for data[3] obtained in the spring of 1950 on

[1] J. R. Macdonald, Phys. Rev. **81**, 312(A), 329(A) (1951).
[2] J. H. E. Griffiths and J. R. Macdonald, J. Sci. Instr. **28**, 56 (1951).
[3] J. R. Macdonald, Ph.D. thesis, Oxford, 1950 (unpublished).
[4] J. H. E. Griffiths, Physica **17**, 253 (1951).
[5] A. F. Kip and R. D. Arnold, Phys. Rev. **75**, 1556 (1949).
[6] J. R. Macdonald, Proc. Phys. Soc. (London) **A64**, 968 (1951).
[7] M. S. Blois, J. Appl. Phys. **26**, 975 (1955).
[8] R. L. Conger and F. C. Essig, Phys. Rev. **104**, 915 (1956).
[9] D. O. Smith, Phys. Rev. **104**, 1280 (1956).